Chemical Geology, 89 (1990) 49–63
Elsevier Science Publishers B.V., Amsterdam — Printed in The Netherlands

[3]

Heavy rare-earth element enrichment in granites of the Aar Massif (Central Alps, Switzerland)

Urs Schaltegger[a,α] and Urs Krähenbühl[b]

[a]*Abteilung für Isotopengeologie, Universität Bern, Erlachstrasse 9a, CH-3012 Bern, Switzerland*
[b]*Laboratorium für Radiochemie, Universität Bern, Freiestrasse 3, CH-3012 Bern, Switzerland*

(Received March 6, 1990; accepted for publication May 30, 1990)

ABSTRACT

Schaltegger, U. and Krähenbühl, U., 1990. Heavy rare-earth element enrichment in granites of the Aar Massif (Central Alps, Switzerland). Chem. Geol., 89: 49–63.

The paper presents rare-earth element (REE) determinations of whole rocks and minerals of the Central Aar Granite, a Hercynian composite granite intrusion in the Aar Massif (Central Alps), consisting mainly of granodiorites, granites and leucogranites. Their geochemical differentation is characterized by a slight depletion of light REE (LREE) and Eu, and a clear enrichment of heavy REE (HREE). This evolution leads to HREE-enriched leucogranites with typical "wing-shaped" distribution patterns in chondrite-normalized diagrams. These distribution patterns can be explained either by pure fractional crystallization of K-feldspar and/or by crystallization of accessory phases that did not deplete the melt in HREE. Due to their affinity to highly polymerized high-silica melts, the latter stayed in the liquid phase until they were incorporated in solids during the final stage of bulk magma crystallization. The REE contents of analyzed mineral phases (allanite, apatite, biotite, epidote, garnet and zircon) are used to calculate a REE budget of the whole rock. These data suggest that existence of further HREE-rich accessory mineral phases in the felsic rock compositions, which have not been analyzed. Qualitative X-ray and EDS analyses revealed the existence of accessory minerals like thorite, chernovite, an Y–Ca mineral and polycrase. These minerals may play an outstanding role in the distribution of REE, U and Th in high-silica melts.

1. Introduction

Quantitative modelling of differentiation processes with rare-earth elements (REE) is a frequently used approach for the understanding of geochemical processes in magmatic rocks. A large amount of published data is available for the calculation of solid/melt partition coefficients ($K_D^{s/l}$) of minerals in ultramafic to intermediate rock compositions. For acid rocks (granites and granodiorites) data on REE contents and partition coefficients of accessory phases (allanite, apatite, monazite, titanite and zircon) are relatively scarce and contradictory (Nagasawa, 1970; Philpotts and Schnetzler, 1970; Arth, 1976; Brooks et al., 1981; Fourcade and Allègre, 1981; Gromet and Silver, 1983; Mahood and Hildreth, 1983; Mittlefehldt and Miller, 1983; Sawka, 1987). Other accessory minerals cannot be included in model calculations because of the lack of published data. Therefore the results of fractional crystallization modelling often contradict the compatible geochemical behaviour of La, Ce and Zr and the incompatible behaviour of Nb, Th, U, Y and Yb, which is characteristic for felsic rock compositions. Other limiting parameters are the inconstancy of $K_D^{s/l}$-values during differentiation (Mahood and Hildreth, 1983) and the lacking knowledge of the com-

[α]*Present address:* Department of Geology, Royal Ontario Museum, 100 Queen's Park, Toronto, Ont. M5S 2C6, Canada.

0009-2541/90/$03.50 © 1990 Elsevier Science Publishers B.V.

plete paragenetic sequence and chemical composition of accessory mineral phases (Sawka, 1987).

The aim of this paper is to describe magmatic geochemical features of REE in Hercynian granites of the Alpine orogen. A data set is presented here that cannot be modelled by simple fractional crystallization of the above-mentioned mineral phases. The paper should provide some insights into REE mineralogy and geochemistry of highly evolved granites.

2. Geology

The Central Aar Granite is a late Westphalian granite body forming the core of the Aar Massif, Central Alps. It consists of several granite subtypes that can be distinguished by their mineralogical and geochemical composition. A short description of the investigated rock types is given in Table I. The different subtypes form a calc-alkaline differentiation suite that is characterized by extreme depletion of Ti, Fe, Mg, P, Ba and Sr, and enrichment of Rb, U, Th, Y and Nb in the most acid members. The main differentiation mechanism was thought to be fractional crystallization of feldspars, biotite, apatite and allanite, but some of the interelement relationships did not agree with this thesis (Schaltegger, 1990a). The granitic melts are characterized by only little crustal contamination and a dominant mantle component. They intruded into the basement rocks after the peak of Hercynian metamorphism and tectonism (Schaltegger, 1989, 1990a).

The investigated granites were subjected to Alpine greenschist-facies metamorphism and to a not yet exactly defined Liassic low-temperature alteration event (Marquer, 1987; Abrecht and Schaltegger, 1988; Schaltegger, 1990b). Alpine metamorphism and deformation caused local mobilization of major and trace elements along 1–10-m-wide deformation zones (Marquer et al., 1985; Marquer, 1987). No mobilization could be detected for REE along strain gradients from isotropic to ultramylonitic stages (Marquer, 1987). Therefore the investigated granites are considered to represent REE contents and distribution patterns that are undisturbed by Alpine metamorphism.

The Liassic hydrothermal alteration caused disturbance of the Rb–Sr whole-rock systems, restricted to the region north of the Grimsel pass (western profile). The lowest Rb–Sr whole-rock ages are around 200–230 Ma (Abrecht and Schaltegger, 1988; Schaltegger, 1989, 1990b). The influence of this event on the REE content of the granites is not known.

3. Investigated material and methods

Eleven samples were taken along two profiles through the Central Aar Granite body (Fig. 1): a western profile following the Grimsel pass road and an eastern profile along the Reuss valley. A short description of the samples and the local names of the different granite subtypes are given in Table I. For detailed petrographic information see Stalder (1964), Labhart (1977) and Schaltegger (1989).

For each sample 20–30 kg of fresh rock material were collected, avoiding zones of Alpine deformation and mineral formation (sericite and epidote). After crushing an aliquot of the whole rock was milled in an agate mill for 15 hr. Heavy-mineral concentrates were obtained using a wet Wilfley table, magnetic separation and heavy liquids (tribromomethane, methylene iodide, N,N-dimethyl formamide). All minerals, except allanite, were separated from two petrographically identical samples (KAW *2519* and *2521*). A pure allanite concentrate could only be obtained from another sample with a similar REE pattern (KAW *2518*). The final mineral samples were hand-picked under the binocular. Grain sizes of > 75 μm were selected to allow hand-picking of all samples; therefore the biotite separate includes inclusions of other minerals that disturb the REE concentrations of the biotite. A short description of the mineral concentrates is given in

TABLE I

Short petrographical description of the analyzed rock samples

Sample No.	Rock name	Mesoscopic description	Mineralogical composition
KAW *128*	Northern Border Facies, Gurtnellen (Reuss valley)	leucocratic, massiv, coarse-grained granite	38% qtz, 35% kfs, 25% plag, 2% bio; ap, op, all, zir, gar, sph, ep, stilp, chl;
KAW *2213*A	Grimsel Granodiorite, Grimsel lake (Grimsel)	dark, coarse-grained granite to granodiorite, strongly foliated in most cases, augen texture; abundant dark enclaves	25% qtz, 25% kfs, 38% plag, 12% bio; ap, op, sph, all, zir, chl, ep, ser, leuc, cc; plag cumulates
KAW *2219*	Central Aar Granite s.s., main facies, Chuenzentennen (Grimsel)	coarse-grained granite with only slight cataclastic deformation	32% qtz, 29% kfs, 31% plag, 8% bio; ap, op, zir, all, leuc, chl, ser, ep
KAW *2220*	Central Aar Granite s.s., leucocratic facies, Hangholz (Grimsel)	medium-grained granite, slightly foliated, occurring as stocks and schlieren within the main facies of the Central Aar Granite s.s.	34% qtz, 32% kfs, 28% plag, 6% bio; ap, op, zir, all, gar, chl, leuc, ser, ep
KAW *2408*	Mittagflue Granite, Tschingel bridge (Grimsel)	leucocratic, massive, coarse-grained granite, analogous to the Northern Border Facies of the Reuss valley	35% qtz, 35% kfs, 28% plag, 2% bio; ap, zir, gar, all, chl, ep, stilp
KAW *2427*	Central Aar Granite s.s., main facies, Gelmerstutz (Grimsel)	coarse-grained, massive granite	main rock-forming minerals as KAW *2219*; op, all, sph, zir, ap, ep, ser
KAW *2518*	Central Aar Granite s.l., Göschenen (Reuss valley)	leucocratic, medium-grained granite, massive to slightly foliated	32% qtz, 32% kfs, 32% plag, 4% bio; ap, ep, all, zir, gar, ser, leuc
KAW *2519*	Central Aar Granite s.l., Schöllenen (Reuss valley)	dark, coarse-grained granodiorite with moderate foliation, augen texture	27% qtz, 35% plag, 28% kfs, 10% bio; all, zir, op, ap, sph, ep, leuc, chl
KAW *2521*	Central Aar Granite s.l. Schöllenen (Reuss valley)	coarse-grained granodiorite, strongly foliated, similar to KAW *2519*	zir, op, ap, sph, ep, leuc, chl same rock-forming minerals as KAW *2519*
KAW *2529*	Kessiturm Aplite, white facies (Grimsel)	fine-grained, aplitic (leucogranitic) intrusion of 200×800 m within the Grimsel Granodiorite	40% qtz, 35% kfs, 24% plag, 1% bio; zir, gar, op, fluo, leuc, chl, ep
KAW *2532*	Kessiturm Aplite, grey facies (Grimsel)	fine-grained grey aplite, forming blobs and schlieren within the white Kessiturm aplite	40% qtz, 30% kfs, 28% plag, 2% bio; gar, chl, ep, ser

Compositions are estimated from thin section. all=allanite; ap=apatite; bio=biotite; cc=calcite; chl=chlorite; ep=epidote; fluo=fluorite; gar=garnet; kfs=K-feldspar; leuc=leucoxene; op=opaques; plag=plagioclase; ser=sericite; sph=sphene; stilp=stilpnomelane; qtz=quartz; zir=zircon.

Table II. To detect a possible REE contamination by the heavy liquids, an ultrapure quartz (Suprasil II®) was analyzed and an aliquot treated with heavy liquids. The detected REE concentrations in the treated quartz powder were negligibly increased thus a blank correction was not applied to the mineral data.

Major- and trace-element data (Table III) were analyzed by standard X-ray fluorescence (XRF) techniques. Analytical description and the full data set of the Central Aar Granite can be found in Schaltegger (1989). REE and Ta (+Hf) have been analyzed by instrumental neutron activation analysis. About 50 mg of the samples (5–50 mg for mineral separates) were irradiated with thermal neutrons for two days at 10^{13} n s^{-1} cm^{-2}. The gamma radiation of the samples was measured three times after

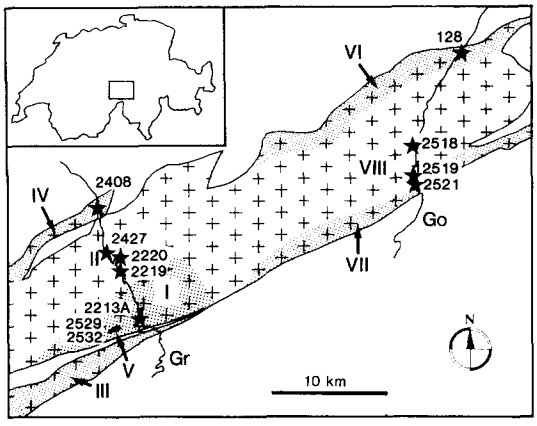


Fig. 1. Geological sketch-map of the central section of the Aar Massif, after Labhart (1977), showing the two investigated profiles. The investigated samples are marked with *asterisks*. Sample AD *26* of Marquer (1987) is close to *2213*A. *Symbols: I*=Grimsel Granodiorite; *II*=Central Aar Granite s.s.; *III*=Southern Aar Granite; *IV*=Mittagflue Granite; *V*=Kessiturm Aplite (all western profile); *VI*=Northern Border Facies; *VII*=Southern Border Facies; *VIII*=central zone (all eastern profile). Aplitic dykes and small leucogranitic stocks are not shown. *Gr*=road over the Grimsel pass, western profile; *Go*=road over the Gotthard pass, Reuss valley (eastern profile).

different waiting periods with a HPGe detector coupled to a loss-free counting system. All concentrations were evaluated relative to those in U.S.G.S. reference materials BCR-*1* and BHVO-*1*. One sigma errors are 5–10% for La, Ce, Eu, Tb and Yb, and 10–15% for Sm, Ta and Hf. For chondrite normalization the results of Leedey chondrite have been taken from Masuda et al. (1973), divided by 1.2 (Taylor and Gorton, 1977).

4. Results

4.1. Geochemical composition of whole rocks

The investigated samples of the Central Aar Granite include granodiorites, granites and leucogranites with SiO_2 contents ranging from 66% to 77% (Table III). The term "leucogranite" is used in a purely descriptive sense for granites containing 5% of mafic minerals (Streckeisen, 1976). These rocks form a calc-alkaline differentiation series, characterized by Fe, Mg, Ti, Ca, P, Sr, Ba depletion and moderate Rb, U, Th, Y, Nb enrichment during differentiation. The leucogranites, i.e. the Mittagflue Granite (KAW *2408*), the Kessiturm Aplite, both western profile (KAW *2529*), and the Northern Border Facies of the eastern profile (KAW *128*) show extremely low contents of Sr, Ba, P and Ti. Major- and trace-element

TABLE II

Description of the analyzed mineral concentrates

Mineral	Grain size	Purity (%)	Description
Allanite	155–200	100	red-brown broken grains, euhedral in thin section; grains always transparent, with darker cores; the sample contains no impurities and no clinozoisite rims; hand-picked
Apatite	75–200	>70	translucent to milky white, stubby prisms; no visible inclusions or zoning; the sample may contain up to 20% of quartz
Biotite	170–250	100	olive-green "books" with no visible mineral intergrowths, but possibly with inclusions of apatite, zircon and opaques; sample hand-picked
Epidote	112–200	100	olive-green anhedral grains, slightly heterogeneous in colour; light-green clinozoisite rims (Alpine metamorphic formation); rarely brownish cores are visible (allanite relics); sample hand-picked
Garnet	155–200	100	pale-orange, euhedral grains with absolutely no inclusions or impurities; sample hand-picked
Zircon	112–115	100	prismatic euhedral crystals, pale-rose to violet; minor inclusions of opaques, no visible zoning, grains with internal turbid zones have been removed by hand
Quartz	75–160		Suprasil II®, ground in an agate micro-mill, washed in 6 *N* HCl bidistilled and triple-distilled water

TABLE III

Major- and trace-element contents of the investigated granitic rocks

Element	KAW *128**	KAW *2213A*	KAW *2219*	KAW *2220*	KAW *2408**	KAW *2427*	KAW *2518*	KAW *2519*	KAW *2529*	KAW *2532*	AD *26*
SiO (wt.%)	75.67	65.91	72.63	72.97	75.84	71.88	70.58	68.08	77.26	74.15	63.73
TiO_2	0.12	0.56	0.23	0.14	0.07	0.27	0.37	0.54	0.07	0.11	0.59
Al_2O_3	15.25	15.39	13.46	12.52	12.38	13.64	14.46	15.52	12.31	14.31	17.38
Fe_2O_3	1.38	3.76	2.23	1.57	1.04	2.13	2.46	3.40	0.69	1.24	3.96
MnO	0.04	0.09	0.07	0.04	0.03	0.09	0.06	0.08	0.05	0.06	0.08
MgO	0.20	0.88	0.29	0.25	0.14	0.49	0.83	1.01	0.23	0.23	1.13
CaO	0.64	2.12	1.21	0.68	0.47	1.10	2.12	2.59	0.41	1.11	2.78
Na_2O	4.01	4.88	4.41	3.81	3.96	4.22	4.05	4.48	3.80	3.91	5.88
K_2O	4.36	3.58	3.87	4.67	4.67	4.32	3.96	3.69	4.63	4.80	3.18
P_2O_5	0.02	0.16	0.06	0.03	0.01	0.07	0.11	0.18	0.01	0.04	0.10
LOI	0.30	1.11	0.52	0.64	0.29	0.59	0.57	0.51	0.21	0.46	0.85
Sum	102.30	98.48	99.03	97.43	98.92	98.79	99.57	100.08	99.67	100.42	99.66
Ba (ppm)	207	1,130	430	367	95	596	1,070	869	43	474	1,219
Rb	200	126	203	207	266	312	138	135	327	246	189
Sr	28	243	75	65	16	116	221	246	10	89	293
Pb	34	22	24	22	33	33	26	30	35	42	n.m.
Th	43	b.d.l.	b.d.l.	b.d.l.	13	9	27	31	43	38	n.m.
U	16	5	12	9	19	18	12	12	18	11	n.m.
Nb	31	17	26	16	32	49	11	15	38	18	29
Y	52	43	56	45	74	129	27	34	82	39	60
Zr	160	325	192	146	106	202	234	278	104	105	321
V	3	50	18	7	b.d.l.	17	30	39	b.d.l.	7	46
Zn	40	65	45	33	22	41	43	55	19	29	n.m.
Sc	5	9	6	4	6	5	5	8	4	5	n.m.
Li	n.m.	17	69	19	11	70	n.m.	n.m.	n.m.	n.m.	n.m.

Data from Schaltegger (1989); sample AD *26* from Marquer (1987). LOI = loss on ignition; b.d.l. = below detection limit; n.m. = not measured.
*Representative analyses of very similar samples.

geochemistry of these rocks is extensively discussed in Schaltegger (1989, 1990a).

The results are plotted into chondrite-normalized variation diagrams (Fig. 2a–c), the data being divided into three groups: (A) granodiorites to granites; (B) granites to microgranites; and (C) leucogranites.

Group A (Fig. 2a) includes the most mafic granitic rocks, i.e. biotite-rich granodiorites and coarse-grained granites (biotite contents 8–15 vol.%) from both profiles (KAW *2213A* and *2519*), but also a medium-grained, more leucocratic granite (KAW *2518*). The sample AD *26* of Marquer (1987) being petrographically and structurally identical with KAW *2213A* has been added, too. The REE patterns of this group are slightly LREE-enriched and show a weak negative Eu anomaly. The range in ΣREE is 263–335 ppm.

Group-B (Fig. 2b) rocks consist of medium- to coarse-grained granites with biotite contents of 4–8 vol.%. The group includes three samples of the Central Aar Granite s.s. (KAW *2219, 2220, 2427*) and the grey type of the Kessiturm Aplite (KAW *2532*), a microgranite intrusion in the Grimsel Granodiorite, all from the western profile (Grimsel). The REE patterns of these rocks are flat and have a moderate negative Eu anomaly. The sample KAW *2427* seems to be anomalous concerning various trace elements: high Li, ΣREE (382 ppm), Rb, Nb, Y, but low Th contents. Its total REE content is nearly twice the mean content (215 ppm) of this group.

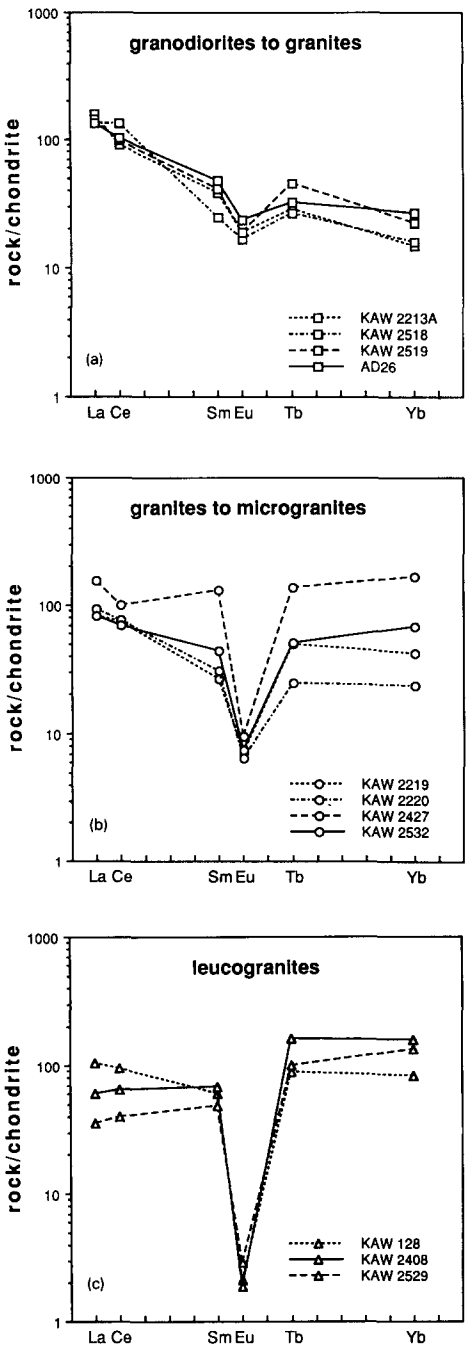


Fig. 2. Chondrite-normalized variation diagrams of REE for the analyzed granites (whole rocks) of the Aar Massif. The REE patterns have been divided in three groups (A, B and C; Fig. 2a, b and c, respectively) showing different REE distribution patterns. The differentiation is characterized by HREE enrichment and Eu and slight LREE depletion.

Group C (Fig. 2c) is formed by leucogranites, i.e. granites with <5 vol.% biotite (Streckeisen, 1976). They occur along the northern border of the Central Aar Granite body, such as the Northern Border Facies (Reuss valley, eastern profile; KAW *128*), the Mittagflue Granite (western profile, Grimsel; KAW *2408*); the group also includes a sample of the white type of the Kessiturm Aplite (western profile; KAW *2529*). REE patterns of these rocks are considerably enriched in HREE and depleted in Eu. The ΣREE range from 159–286 ppm.

The REE contents of the ten analyzed whole-rock samples cover a range of 159–382 ppm (Table IV: ΣREE obtained by interpolation of the known values). ΣREE is not clearly correlated with SiO_2 contents (Fig. 3a), but the light REE (LREE), e.g. La, as well as the heavy REE (HREE), e.g. Yb, exhibit clear negative and positive correlations, respectively (Fig. 3b and c). They evidence the depletion of LREE and the enrichment of HREE during differentiation. The geochemical behaviour of HREE (Yb) is identical with Y, the latter being also enriched during differentiation (Schaltegger, 1990a). Ta is known as incompatible element in granitic rock suites (Fourcade and Allègre, 1981; Henderson, 1982) but shows no distinct enrichment. The degree of negative Eu anomaly is strongly correlated with the Ce/Yb ratio (Fig. 3d). The positive correlation between Eu and Sr (Fig. 3e) argues for feldspar separation from the melt.

4.2. REE *contents of accessory minerals*

4.2.1. Allanite. It is a very common accessory mineral in granitic rocks and may contain large amounts of REE, especially LREE. The interpolated ΣREE content of KAW *2518* allanite is ~23%, La and Ce ~11%, the LREE, especially Ce, being stoichiometric constituents of the allanite lattice. The whole-rock-normalized pattern of the analyzed allanite concentrate agrees well with data from literature

TABLE IV

Contents (in ppm) of La, Ce, Sm, Eu, Tb, Yb, Lu, Ta and Hf in whole rocks and minerals of the Central Aar Granite

Sample name	La	Ce	Sm	Eu	Tb	Yb	Lu	Eu/Eu*	ΣREE	Ta	Hf
Whole rocks:											
KAW *128*	33	78	11.4	0.15	4.3	17	0.89	0.017	286	2.5	7.7
*KAW 2213*A	50	74	7.2	1.36	1.4	3.1	1.3	0.26	263	4.1	9.5
KAW *2219*	26	61	5.1	0.51	2.4	8.6	11.9	0.12	218	7.1	7.2
KAW *2220*	29	63	5.9	0.47	1.2	4.9	3.4	0.11	214	6.5	6.0
KAW *2408*	19	52	13.0	0.14	8.0	33	6.8	0.012	239	7.2	6.1
KAW *2427*	49	82	24.9	0.69	6.7	35	10.1	0.037	382	9.8	10.1
KAW *2518*	42	108	4.7	1.20	1.3	3.3	n.m.	0.34	335	1.4	7.6
KAW *2519*	45	79	7.8	1.35	2.2	4.6	0.53	0.23	275	3.5	7.2
KAW *2529*	11	32	9.2	0.21	4.9	28	6.0	0.027	159	5.7	6.5
KAW *2532*	26	57	8.4	0.54	2.5	14	3.1	0.084	214	3.5	4.3
AD *26*	42	84	9.1	1.68	1.6	5.4	0.96	0.25	303	3.3	n.m.
Minerals:											
KAW *2518* allanite	32,500	78,700	1,760	50	127	64	n.m.	0.041	234,626	6.4	10
KAW *2519* apatite	48	125	28	1.7	6.3	12	n.m.	0.079	476	0.84	19
KAW *2519* biotite	680	970	42	1.5	4.7	11	n.m.	0.050	3,255	8.0	22
KAW *2521* epidote	735	995	168	9.3	34	110	n.m.	0.075	3,884	23	11
KAW *2521* garnet	9.5	67	2.8	0.48	0.9	298	n.m.	0.22	780	0.83	32
KAW *2521* zircon	57	426	154	b.d.	23	630	n.m.	<0.001	2,857	5.7	11,400
Quartz, clean	0.20	0.33	0.04	0.004	0.02	0.02	n.m.			0.015	0.16
Quartz, heavy liquids	0.34	0.42	0.02	0.007	0.02	0.02	n.m.			0.008	0.22

Eu* was obtained by linear interpolation between Sm and Tb. Total REE (ΣREE) contents were calculated after interpolation of the contents of the undetermined REE. Because of poor analytical reproducibility, the Lu values are not used for diagrams but given for information only; n.m. = not measured; b.d.l. = below detection limit. Sample AD *26* from Marquer (1987).

(Brooks et al., 1981; Gromet and Silver, 1983) for both LREE and HREE (Fig. 4a). However, KAW *2518* allanite shows a negative Eu anomaly and contains 60× more LREE than the LREE-richest coexisting mineral (epidote). Allanite is a liquidus phase in all investigated rocks and occurs as euhedral crystals; its modal abundance is estimated to be 0.1 vol.%. All estimations on modal abundances are means of the three samples KAW *2518, 2519* and *2521*.

4.2.2. Apatite. The analyzed mineral concentrate shows low ΣREE, slightly above whole-rock values. The pattern (Fig. 4b) is flat, with a negative Eu anomaly. The ΣREE of 476 ppm is by a factor of 10–20 lower than other published values (Nagasawa, 1970; Fourcade and Allègre, 1981; Gromet and Silver, 1983). This value may be influenced by some 20% addition of quartz to the apatite. The compilation of published apatite data in Fig. 4b reveals the large variation in both contents and shape of the REE patterns, eventually indicating variations in $K_D^{s/l}$-values. Apatite occurs as subhedral to euhedral crystals, mostly included in biotite; its modal whole-rock content is 0.3 vol.%.

4.2.3. Biotite. The analyzed sample is extremely high in ΣREE, strongly enriching the LREE (see Fig. 4c). K_D-values for biotites are considered to be less than unity for all REE, thus low ΣREE may be expected (Hanson, 1978). The high abundances may be due to impurities such as inclusions of allanite, apatite, opaques and zircon. The biotite of Fourcade and Allègre (1981) from a biotite granite (Qt *15*) shows elevated REE values as well, but

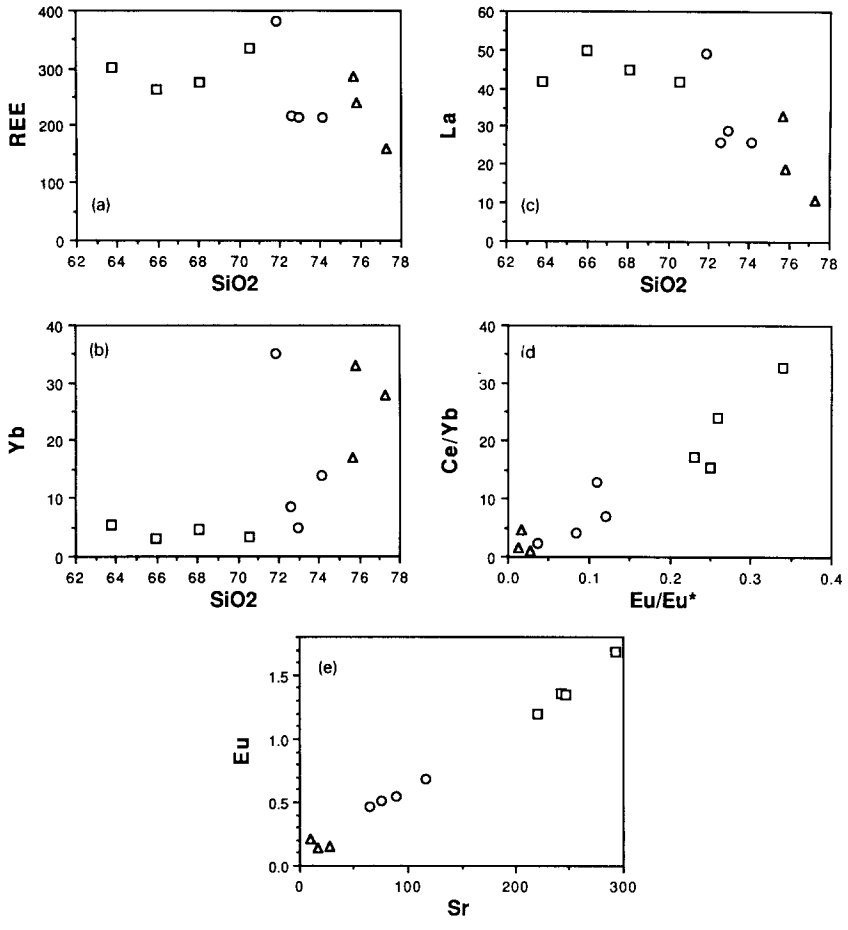


Fig. 3. a–c. Harker diagram of whole rocks for total REE [ΣREE; (a)], Yb (b) and La (c) contents. Yb and La show a clear dependence from SiO_2 content, whereas ΣREE show no distinct systematics.
d. Ce/Yb–Eu/Eu* diagram of whole-rock analyses. Both the LREE/HREE and feldspar fractionation must have acted at the same time, yielding a linear trend in this diagram.
e. Eu–Sr diagram of whole-rock analyses. The positive correlation indicates feldspar fractionation from the melt. Same *symbols* for the group *A–C* rocks as in Fig. 2.

no enrichment of LREE. Biotites from acid rocks may eventually have partition coefficients above unity. KAW *2519* biotite has a marked Eu anomaly which seems to be common in granitic biotites (see, e.g., Fourcade and Allègre, 1981). Whole-rock LREE contents calculated with the KAW *2518* biotite data and its modal abundance (8 vol.%) exceed 100%, evidencing the presence of contaminating phases in the analyzed mineral concentrate.

4.2.4. Epidote. Beside allanite, epidote is the REE-richest mineral of the investigated granite samples. Its REE pattern is flat and has a negative Eu anomaly (Fig. 4a). Gromet and Silver (1983) described magmatically grown epidote in a granodiorite that shows considerably lower REE contents than KAW *2521* epidote. The result may be biased by the selection of dark-green grains of equal colour: these grains may have formed from allanite or even contain relics of allanite, whereas light-green, perfectly transparent grains may represent an Alpine metamorphic formation from the anorthite component of the plagioclases (clino-

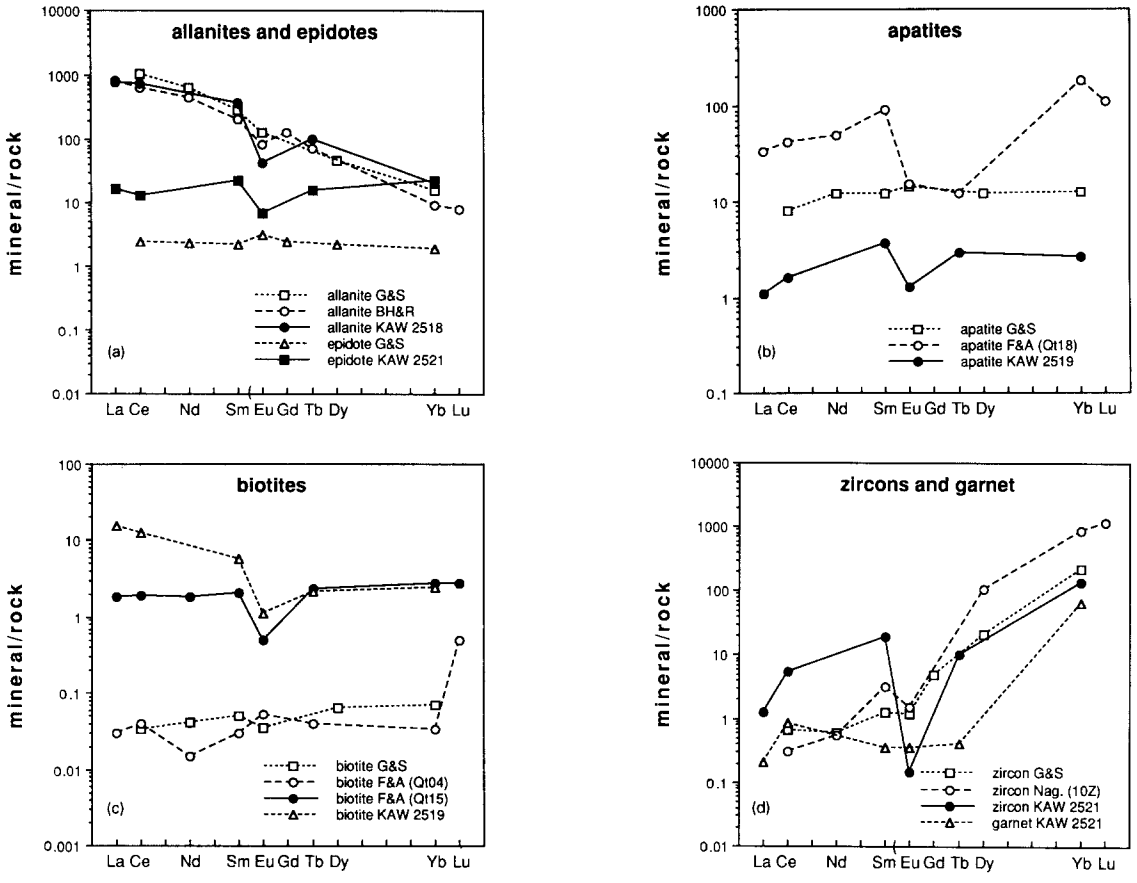


Fig. 4. Whole-rock normalized variation diagrams of REE for the analyzed mineral concentrates, compared to REE patterns from literature.
a. REE patterns of allanites from Brooks et al. (1981), and Gromet and Silver (1983), compared to KAW *2518* allanite, and of an epidote of Gromet and Silver (1983) and KAW *2521* epidote.
b. REE patterns of KAW *2519* apatite and apatites from Fourcade and Allègre (1981), and Gromet and Silver (1983).
c. REE patterns of KAW *2519* biotite and biotites of Fourcade and Allègre (1981), and Gromet and Silver (1983).
d. REE pattern of KAW *2521* zircon, compared to data of Nagasawa (1970), and Gromet and Silver (1983), and pattern of KAW *2521* garnet.

zoisite). Its modal abundance is estimated to be 0.3 vol.%.

4.2.5. Garnet. The analyzed fraction of pale-orange euhedral crystals shows a strong preferency for HREE and slightly enhanced Ce values (Fig. 4d). The ΣREE content of the analyzed garnet is 780 ppm, thus with an estimated modal abundance of 0.02 vol.% its contribution to the whole-rock REE content is minute. The analyzed orange Mn- and Ca-rich garnets of the Central Aar Granite are considered to be a product of Alpine metamorphism (Steck and Burri, 1971). This result argues for some mobility of REE during Alpine metamorphism, which is also indicated by the presence of REE minerals in Alpine mineral fissures.

4.2.6. Zircon. It is known as the main HREE-containing accessory mineral in granites. K_D-values are in the range of 4 for LREE and 140–350 for HREE (Henderson, 1982). The analyzed zircon from sample KAW *2521* shows whole-rock-normalized LREE contents that are

10× higher than the selected examples from literature (Nagasawa, 1970; Gromet and Silver, 1983), see Fig. 4d, but similar HREE contents. The analyzed Eu content has been below detection limit (<0.2 ppm) thus a strong negative Eu anomaly results. The U content of a similar zircon concentrate of KAW *2519* is 1200 ppm (Schaltegger and Quadt, 1990). Its modal abundance is estimated as 0.1%.

The analyzed zircons have small amounts of opaque and abundant acicular apatite inclusions, which might contribute to the phenomenon of the observed LREE enrichment. Qualitative energy-dispersive X-ray fluorescence (EDS) microprobe analyses evidenced the presence of U–Th silicates as inclusions in zircons, that may have a strong preferency for LREE.

5. Interpretation of the whole-rock REE patterns

5.1. Parent melts

It is assumed that the rocks of the Central Aar Granite evolved from a source magma whose composition was more basic than the investigated granodiorites (KAW *2213*A, *2519*, *2521*). The latter, considered as differentiates of a probably low crustal magma chamber, have slightly LREE-enriched patterns with a weak negative Eu anomaly. Statements about the differentiation mechanism from the source magma can only be speculative. Nevertheless an episode of fractional crystallization of hornblende and plagioclase must be envisaged to produce granodioritic rocks from a possible dioritic source. However, extensive fractional crystallization of hornblende would lead to low HREE concentration in the granitic melts, which is not the case. Hornblende crystallization must consequently have been a subordinate process and/or the hypothetical dioritic source was already enriched in HREE.

5.2. Behaviour of REE *during differentiation*

During differentiation from intermediate to more acid compositions, LREE are normally enriched or slightly depleted and HREE and Eu strongly depleted (see, e.g., Emmermann et al., 1975). The investigated granites of the Central Aar Granite body show an "anomalous" behaviour of the REE: With increasing acidity LREE and Eu are depleted, HREE are enriched (Fig. 3b and c). Fractionation of LREE in felsic rock seems to be quite common and has been attributed to monazite or allanite crystallization (Miller and Mittlefehldt, 1982; Mittlefehldt and Miller, 1983). Monazite has never been observed in the investigated rocks thus fractionation of small amounts of allanite is responsible for the slight LREE depletion. The increasing negative Eu anomaly is in agreement with feldspar fractionation evidenced by drastic depletion of Ba and Sr (Schaltegger, 1989, 1990a; see Fig. 3e). In fact all analyzed minerals show a negative Eu anomaly, which indicates high oxygen fugacity throughout the whole crystallization sequence.

Flat or slightly HREE-enriched granite patterns with extreme Eu anomalies, such as leucogranites of Fig. 2c, are known from several two-mica granites and leucogranites of the European Hercynides (Fourcade and Allègre, 1981; Cocherie, 1984; Webb et al., 1985). These patterns are normally coupled with low ΣREE concentrations, considerably below 100 ppm. This is not the case with the investigated leucogranites. Two possible mechanism could explain these HREE enrichments: (1) enrichment during a post-magmatic fluid–rock interaction with F-bearing fluids that are thought to form complexes of HREE, together with Na, Nb, Y, Zr, Hf, Ta and U (Webb et al., 1985), and (2) magmatic enrichment in a high-silica melt with fractional crystallization of mineral phases that have $K_D^{LREE} \geqslant 1$ and $K_D^{HREE} < 1$.

An intensive fluid–rock interaction in the felsic granites of the western profile (Grimsel) is evidenced by disturbed Rb–Sr whole-rock

systems (Schaltegger, 1989, 1990b). Such an alteration might lead to the precipitation of REE, Ta, Y, Nb and U minerals or to in situ alteration of pre-existing accessory phases (Cathelineau, 1988). Both effects have not been detected in thin section. In the corresponding rocks of the Reuss valley showing the same HREE enrichments, only little disturbance of the Rb–Sr whole-rock systems has been found, thus a fluid-induced tilting of the REE-patterns is unlikely.

In the investigated granite suite the HREE enrichment is strongly correlated with increasing SiO_2 content (Fig. 3b) and increasing negative Eu anomaly (Fig. 3d). This fact favours a magmatic process which must have acted parallel to the fractional crystallization of feldspars. Mittlefehldt and Miller (1983) modelled melt compositions with "wing-shaped" REE patterns and enriched HREE assuming pure fractional crystallization of feldspars. This hypothesis could explain the perfect fit of data in a Ce/Yb–Eu/Eu* diagram (Fig. 3d). Because no HREE-favouring mineral was formed in the magma, such as hornblende (K_D^{HREE} 3–9) or garnet (K_D^{HREE} 7–43; data from Henderson, 1982), the main portion of HREE remained in the melt phase. Fractional crystallization of zircon and sphene were subordinate processes and did not decrease the HREE concentration of the residual melts, which consequently enriched Nb, Y and HREE.

This enrichment can be interpreted in terms of increasing melt polymerization, which causes the HREE to stay preferentially in the melt as network-modifying elements in octahedral sites (Mahood and Hildreth, 1983), whereas the smaller REE cations tend to be incorporated in minerals.

6. Interpretation of the mineral data

The REE determinations of six different mineral phases from the Central Aar Granite should allow an estimate about the distribution of REE among rock-forming and accessory minerals of the investigated granites. For a REE rock budget (Fig. 5) modal abundances have been estimated from thin-section observation and trace-element contents of the whole rock, assuming that all La is in allanite, all P in apatite and all Zr in zircon. Biotite has been excluded from Fig. 5 because of its anomalous contents of LREE, which are due to impurities. The phases plagioclase, K-feldspar and titanite have not been determined. Other accessory phases, mainly occurring in the more felsic rock compositions, are fluorite, galena, ilmenite, sphalerite, molybdenite and thorite; hematite is of Alpine metamorphic origin.

The shapes of curves in Fig. 5 are equivalent to whole-rock-normalized distribution patterns. The Ca-silicates allanite and epidote clearly show the highest REE contents of all analyzed minerals. With modal abundances of 0.1 and 0.3 vol.%, respectively, they contribute most to the REE whole-rock budget, especially for LREE. Apatite shows a slightly concave pattern which is in agreement with apatite/matrix distribution curves (Naga-

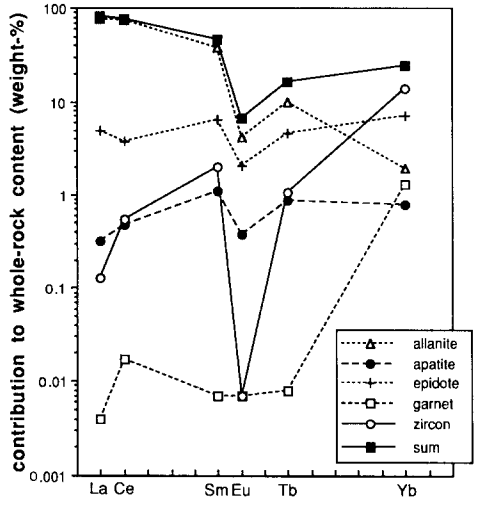


Fig. 5. Fractional contribution of each mineral to whole-rock REE contents, given as wt.%. The shapes of the patterns are equivalent to whole-rock normalized variation curves. Biotite is not shown because of impurities in the analyzed mineral concentrate. The five analyzed mineral phases contribute up to 83% of LREE, but only 25% of Yb. It is assumed that other HREE-rich phases may exist in the analyzed granites.

sawa, 1970) as well as with experimental results (Watson and Green, 1981). Its low total REE content may be explained by the paragenetic sequence in the investigated rocks: the crystallization of allanite, zircon and small amounts of titanite may have lowered the overall REE content of the melt prior to apatite crystallization; therefore the mineral/melt partition coefficients for apatite became small (see Sawka, 1987). Zircon commonly contributes a great part of HREE, but the analyzed zircon sample is a main carried of LREE, too. Hildreth (1979) reports variable LREE contents in zircons of high-silica portions of the Bishop Tuff, California, U.S.A., giving maximal Ce/Yb values up to 3.7 and mineral/whole rock partition coefficients for Ce up to 23! This variable mineral/whole rock partition argues for increasing $K_D^{s/l}$-values with increasing degree of differentiation and melt polymerization (Mahood and Hildreth, 1983). In the case of KAW *2521* zircon, however, opaque inclusions might cause its anomalous LREE contents. Garnet concentrates HREE as well but cannot contribute > 1% of the whole-rock Yb content due to its low modal abundance.

The mineral phases allanite, apatite and zircon could theoretically be inherited crystals (cumulus phases) of a former magmatic stage or residual phases of source rocks. In both cases they would not be in equilibrium with melt. The lack of a considerable component of inherited Pb in the zircons (Schaltegger and Quadt, 1990) argues for the melts being undersaturated in Zr. For KAW *2518, 2519* and *2521* zircon saturation occurs at temperatures of 780–790°C (Watson and Harrison, 1983), which seems rather high for melts of granodioritic to granitic composition. The zircons crystallized during subsequent cooling and are in equilibrium with the melt in which they occur. The P_2O_5 content of the whole rocks is decreasing with increasing SiO_2 contents. This fact argues for the removal of P_2O_5 through apatite crystallization, thus apatite saturation was achieved throughout the whole differentiation process (Green and Watson, 1982). Epidote and garnet are both considered as Alpine neoformations and should therefore not be used for a primary magmatic element budget. However, both minerals are secondary products of magmatic mineral phases (allanite, plagioclase, biotite) and may have incorporated the main proportion of REE of their sources. The analyzed accessory mineral spectrum thus consists of various generations of magmatic and metamorphic phases.

The data of Fig. 5 reveal that the five minerals allanite, apatite, epidote, garnet and zircon contribute 83% of the whole-rock La and 73% of the Ce, but only 16% of the Tb and 25% of the Yb. The same holds for U, only 10% of its whole-rock content being supplied by zircon. This evidences that major HREE, U-rich accessory phases have not been detected in these rocks. Titanite is of minor importance in this question because its modal abundance is < 0.1%.

Late-stage minerals that may incorporate HREE, U and Th have been detected in the high-silica leucogranites: X-ray determinations of a brown mineral grain in the heavy concentrate of the Mittagflue Granite lead to the provisional identification of chernovite (YAs_4). Qualitative EDS microprobe and SEM (scanning electron microscope) analyses evidenced the presence of an Y–Ca mineral (Y-carbonate?) in KAW *2220* and considerable amounts of U-, Fe-, Pb- and P-bearing thorite in KAW *2220, 2408* and *2518*, in the case of KAW *2408* exceeding by far the abundance of zircon. Because thorite is significantly enriched in the leucogranites, it preferentially crystallized in the late high-silica melts. The euhedral crystal shape (Fig. 6) reveals its early formation in the paragenetic sequence of these rocks. Bajo et al. (1983) reported the presence of polycrase (Y,REE,U,Th,Ca)- $(Nb, Ta, Ti, Fe)_2O_6$, thorite and possibly other U- and Th-silicates in the Mittagflue Granite. The accessory mineralogy of granites may even be more complex: Silver et al. (1980) describe the

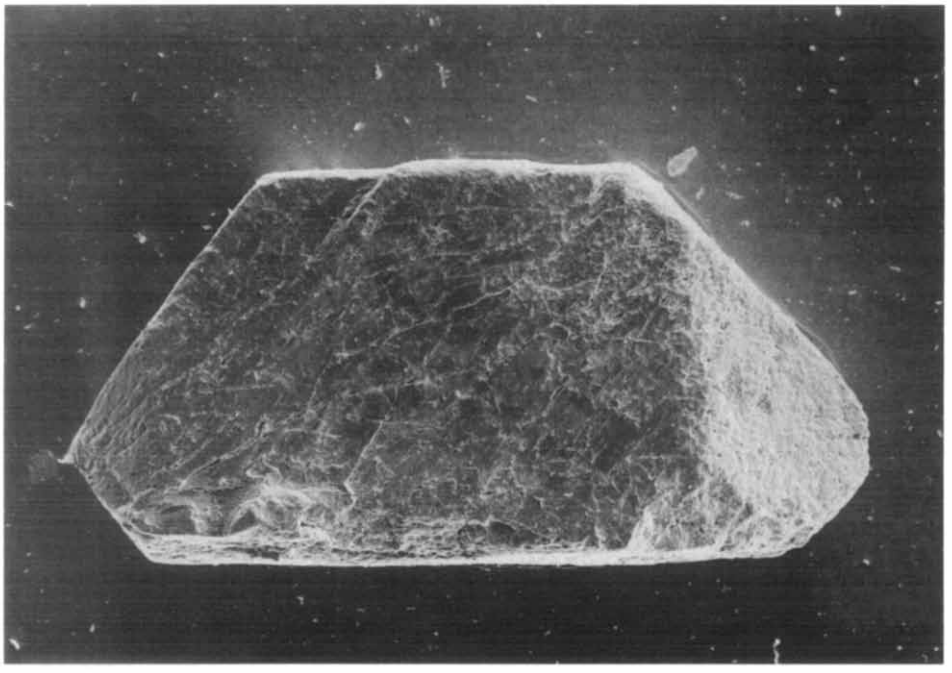


Fig. 6. SEM image of an euhedral thorite in the Mittagflue Granite (KAW *2408*); magnification 175×.

presence of brannerite, coffinite, thorite and xenotime beside the more common accessory phases in a granite. Some of these minerals may incorporate several percent of REE, especially HREE, U and Th. Bajo et al. (1983) report U contents of 8% and Th contents of 30% for opaque impurities in zircons from the Mittagflue Granite, as well as high portions of extractable U and Th, which may be located on grain boundaries.

7. Summary and conclusions

The results of the Central Aar Granite do not allow statements about its source melts and their evolution towards granodioritic and granitic rocks. The REE distribution patterns are completely dominated by the late-stage fractional crystallization processes. The observed REE patterns of granodiorites, granites and leucogranites of the Central Aar Granite are compatible with element fractionation from a melt; an influence of fluid–rock interaction can be excluded. The shape of the whole-rock patterns changes with the degree of differentiation and is clearly correlated with major- and trace-element contents. The geochemical evolution is characterized by a slight depletion of LREE and an enrichment of the HREE; therefore, it is evident that REE change their geochemical behaviour during differentiation in high-silica melts: LREE become compatible and are removed by allanite (or monazite, not detected in the present study) crystallization whereas HREE are enriched in the liquid phase (Miller and Mittlefehldt, 1982; Mahood and Hildreth, 1983). The increasing negative Eu anomaly can be explained by fractional crystallization of feldspars. Both LREE/HREE fractionation and Eu depletion have to be parallel processes or might be explained by fractional crystallization of feldspars (see Mittlefehldt and Miller, 1983), or by crystallization of a combination of rock-forming and small amounts of accessory mineral phases. All the discussed fractional crystallization processes did not deplete the melt in HREE, U and Th, thus the crystallization of allanite and zircon

must have played a minor role in the evolution of the melt. The HREE-enriched leucogranites require the presence of HREE-rich minerals, other than the analyzed accessory phases (allanite, apatite, epidote, garnet and zircon).

The determined REE contents of allanite, apatite, epidote, garnet and zircon, compared to published data, reveal the enormous variation in both REE concentrations and distribution patterns of several minerals. Strong variations of whole-rock-normalized REE abundances argue for different $K_D^{s/l}$-values in different melt compositions. The variation of the REE contents of biotite could point to mineral separation problems, biotite being known as host for REE-rich accessory minerals.

The HREE-enriched felsic rocks (leucogranites) must contain considerable amounts of accessory phases that may incorporate HREE at the percent level. Among these U–Th-silicates, chernovite, polycrase and an unspecified Y–Ca phase have been qualitatively determined. Model calculations of fractional crystallization in felsic melts should consider these accessory phases as well as appropriate K_D-values for each mineral and melt composition.

Acknowledgements

We would like to thank both the staff of the Laboratorium für Radiochemie and the Abteilung für Isotopengeologie of the University of Bern for their support and technical assistance. F. Zweili, Geologisches Institut, kindly made SEM images and EDS analyses of grain mounts. The paper was substantially improved by discussions and comments of B. Bonin, Paris; M. Flisch, Bern; and F. Corfu and S. Noble, Toronto. The Schweizerischer Nationalfonds is greatfully acknowledged for financially supporting the infrastructure of the Abteilung für Isotopengeologie.

References

Abrecht, J. and Schaltegger, U., 1988. Aplitic intrusions in the central Aar massif basement: geology, petrography and Rb–Sr data. Eclogae Geol. Helv., 81: 227–239.

Arth, J.G., 1976. Behaviour of trace elements during magmatic processes – a summary of theoretical models and their applications. J. Res. U.S. Geol. Surv., 4(1): 41–47.

Bajo, C., Rybach, L. and Weibel, M., 1983. Extraction of uranium and thorium from Swiss granites and their microdistribution, 2. Microdistribution of uranium and thorium. Chem. Geol., 39: 299–318.

Brooks, C.K., Henderson, P. and Ronsbø, J.G., 1981. Rare-earth partition between allanite and glass in the obsidian of Sandy Braes, Northern Ireland. Mineral. Mag., 44: 157–160.

Cathelineau, M., 1988. Accessory mineral alteration in peraluminous granites at the hydrothermal stage: a review. Rend. Soc. Ital. Mineral. Petrogr., 43: 499–508.

Cocherie, A., 1984. Interaction manteau–croûte: son rôle dans la genèse d'associations plutoniques calco-alcalines, contraintes géochimiques (élements en traces et isotopes du strontium et de l'oxygène). Doc. Bur. Rech. Géol. Min., Paris, 90, 246 pp.

Emmermann, R., Daieva, L. and Schneider, J., 1975. Petrologic significance of rare earth element distribution in granites. Contrib. Mineral. Petrol., 52: 267–283.

Fourcade, S. and Allègre, C.J., 1981. Trace element behaviour in granite genesis – A case study – The calc-alkaline plutonic association from the Quérigut Complex (Pyrénées, France). Contrib. Mineral. Petrol., 76: 177–195.

Green, T.H. and Watson, E.B., 1982. Crystallization of apatite in natural magmas under high pressure, hydrous conditions, with particular reference to 'orogenic' rock series. Contrib. Mineral. Petrol., 79: 96–105.

Gromet, L.P. and Silver, L.T., 1983. Rare earth element distribution among minerals in a granodiorite and their petrogenetic implications. Geochim. Cosmochim. Acta, 47: 925–939.

Hanson, G.N., 1978. The application of trace elements to the petrogenesis of igneous rocks of granitic composition. Earth Planet. Sci. Lett., 38: 26–43.

Henderson, P., 1982. Inorganic Geochemistry. Pergamon, Oxford, 353 pp.

Hildreth, W., 1979. The Bishop Tuff: Evidence for the origin of compositional zonation in silicic magma chambers. U.S. Geol. Surv., Spec. Pap. No. 180.

Labhart, T.P., 1977. Aarmassiv und Gotthardmassiv. Sammlg. Geol. Führer, 63. Bornträger, Berlin, 173 pp.

Mahood, G. and Hildreth, W., 1983. Large partition coefficients for trace elements in high-silica rhyolites. Geochim. Cosmochim. Acta, 47: 11–30.

Marquer, D., 1987. Transfert de matière et déformation

progressive des granitoïdes – Exemple des massifs de l'Aar et du Gothard (Alpes Centrales Suisses). Mém. Doc. Cent. Armoricain Étude Struct. Socles, Rennes, 10, 287 pp.

Marquer, D., Gapais, D. and Capdevila, R., 1985. Comportement chimique et orthogneissification d'une granodiorite en faciès schistes verts (Massif de l'Aar, Alpes Centrales). Bull. Minéral., 108: 209–221.

Masuda, A., Nakamura, N. and Tanaka, T., 1973. Fine structures of mutually normalized rare-earth patterns of chondrites. Earth Planet. Sci. Lett., 37: 239–248.

Miller, C.F. and Mittlefehldt, D.W., 1982. Depletion of light rare-earth elements in felsic magmas. Geology, 10: 129–133.

Mittlefehldt, D.W. and Miller, C.F., 1983. Geochemistry of the Sweetwater Wash Pluton, California: Implications for "anomalous" trace element behaviour during differentiation of felsic magmas. Geochim. Cosmochim. Acta, 47: 109–124.

Nagasawa, H., 1970. Rare earth concentrations in zircons and apatites and their host dacites and granites. Earth Planet. Sci. Lett., 9: 359–364.

Philpotts, J.A. and Schnetzler, C.C., 1970. Phenocryst–matrix partition coefficients for K, Rb, Sr and Ba with applications to anorthosite and basalt genesis. Geochim. Cosmochim. Acta, 34: 307–378.

Sawka, W.N., 1987. REE and trace element variations in accessory minerals and hornblende from the strongly zoned McMurry Meadows Pluton, California. Trans. R. Soc. Edinburgh, 97: 157–168.

Schaltegger, U., 1989. Geochemische und isotopengeochemische Untersuchungen am Zentralen Aaregranit und seinen assoziierten Gesteinen zwischen Aare und Reuss (Aarmassiv, Schweiz). Ph.D. Thesis, University of Bern, Bern (unpublished).

Schaltegger, U., 1990a. The Central Aar Granite: Highly differentiated calc-alkaline magmatism in the Aar Massif (Central Alps, Switzerland). Eur. J. Mineral., 2: 245–259.

Schaltegger, U., 1990b. Post-magmatic resetting of Rb–Sr ages – a study in the Central Aar Granite (Central Alps, Switzerland). Geol. Rundsch., 79(3): 709–724.

Schaltegger, U. and Quadt, A., 1990. U–Pb zircon dating of the Central Aar Granite (Central Alps, Switzerland). Schweiz. Mineral. Petrogr. Mitt. (in press).

Schnetzler, C.C. and Philpotts, J.A., 1970. Partition coefficients of rare-earth elements between igneous matrix material and rock-forming mineral phenocrysts, II. Geochim. Cosmochim. Acta, 34: 331–340.

Silver, L.T., Williams, I.S. and Woodhead, J.A., 1980. Uranium in granites from the southwestern United States: Actinide parent–daughter systems, sites and mobilization. First Year Rep., U.S. Dep. Energy, Washington, D.C., 380 pp.

Stalder, H.A., 1964. Petrographische und mineralogische Untersuchungen im Grimselgebiet. Schweiz. Mineral. Petrogr. Mitt., 44: 187–398.

Steck, A. and Burri, G., 1971. Chemismus und Paragenesen von Granaten aus Granitgneisen der Grünschiefer- und Amphibolitfazies der Zentralalpen. Schweiz. Mineral. Petrogr. Mitt., 51: 534–538.

Streckeisen, A., 1976. To each plutonic rock its proper name. Earth-Sci. Rev., 12: 1–33.

Taylor, S.R. and Gorton, M.P., 1977. Geochemical application of spark source mass spectrography, III. Element sensitivity, precision and accuracy. Geochim. Cosmochim. Acta, 41: 1375–1380.

Watson, E.B., 1979. Zircon saturation in felsic liquids: Experimental results and applications to trace element geochemistry. Contrib. Mineral. Petrol., 70: 407–419.

Watson, E.B. and Green, T.H., 1981. Apatite/liquid partition coefficients for the rare earth elements and strontium. Earth Planet. Sci. Lett., 56: 405–421.

Watson, E.B. and Harrison, T.M., 1983. Zircon saturation revisited: temperature and composition effects in a variety of crustal magma types. Earth Planet. Sci. Lett., 64: 295–304.

Webb, P.C., Tindle, A.G., Barrit, S.D., Brown, G.C. and Miller, J.F., 1985. Radiothermal granites of the United Kingdom: comparison of fractionation patterns and variation of heat production fro selected granites. In: High Heat Production (HHP) Granites, Hydrothermal Circulation and Ore Genesis. Inst. Min. Metall., London, pp. 409–424.